

Progress reports on:

**Finite- β Three-Dimensional MHD Equilibrium
Studies**

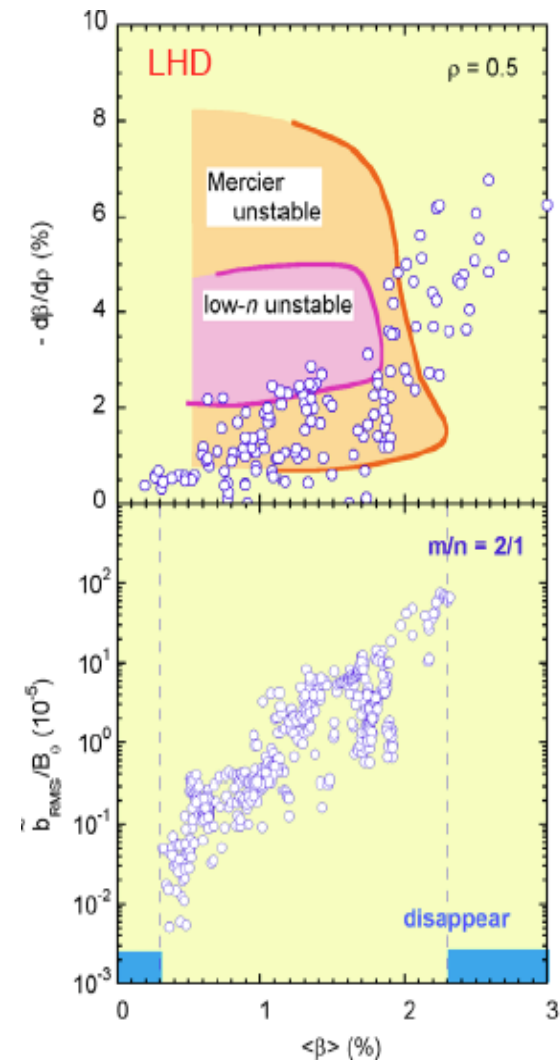
M. Schlutt, C. C. Hegna, E. D Held

Resistive Wall Mode/Field Error Penetration Physics

A. Montgomery, A. J. Cole, C. C. Hegna, S. E. Kruger

Recent stellarator experiments motivate the need for high β MHD equilibrium studies

- In LHD, low- m/n instabilities are observed --- similar in W7X
 - Onset largely in accord with theory
 - Mode grows, benignly, no disruptions
- In contrast to tokamak, where ideal β -limit is extensively studied --- upper limit invariably leads to disruption
- 3-D MHD equilibrium physics may produce limit on stellarator β .
 - Pressure induced currents degrade magnetic surface integrity?
 - Degradation typically occurs via the production of 'weakly' stochastic edge magnetic fields --- self-consistent transport physics?



NIMROD will be used to study finite- β physics in 3-D geometry --- M. Schlutt et al

- Straight stellarator studies --- pure helically symmetric vacuum states in periodic cylinder geometry
 - Vary vacuum by adding 'weak' 3-D magnetic fields ---> Produces magnetic islands, weak stochasticity.
 - Add heating source --- produce pressure profile
 - Transport properties (parallel and perpendicular) affect the pressure profile formation.
 - Self-consistent pressure induced currents using a resistive MHD model
 - Anisotropic heat transport --- ultimately, integral closure techniques for parallel heat conduction
 - Coupled to analytic theory modeling --- resistive MHD

Simulations start from vacuum solutions to the magnetic field

- Vacuum solutions to the magnetic field in periodic cylinder geometry are given by

$$\vec{B} = \nabla\varphi, \quad \nabla^2\varphi = 0,$$

$$\varphi = B_0 \left[R\xi + \sum_{m,n} \varepsilon_{mn} \frac{Rm}{n} I_m \left(\frac{nr}{R} \right) \sin(m\theta - n\xi) \right]$$

- $z = R\xi$, $I_m =$ modified Bessel function
- Shape and spectrum of magnetic fields controlled by choice of

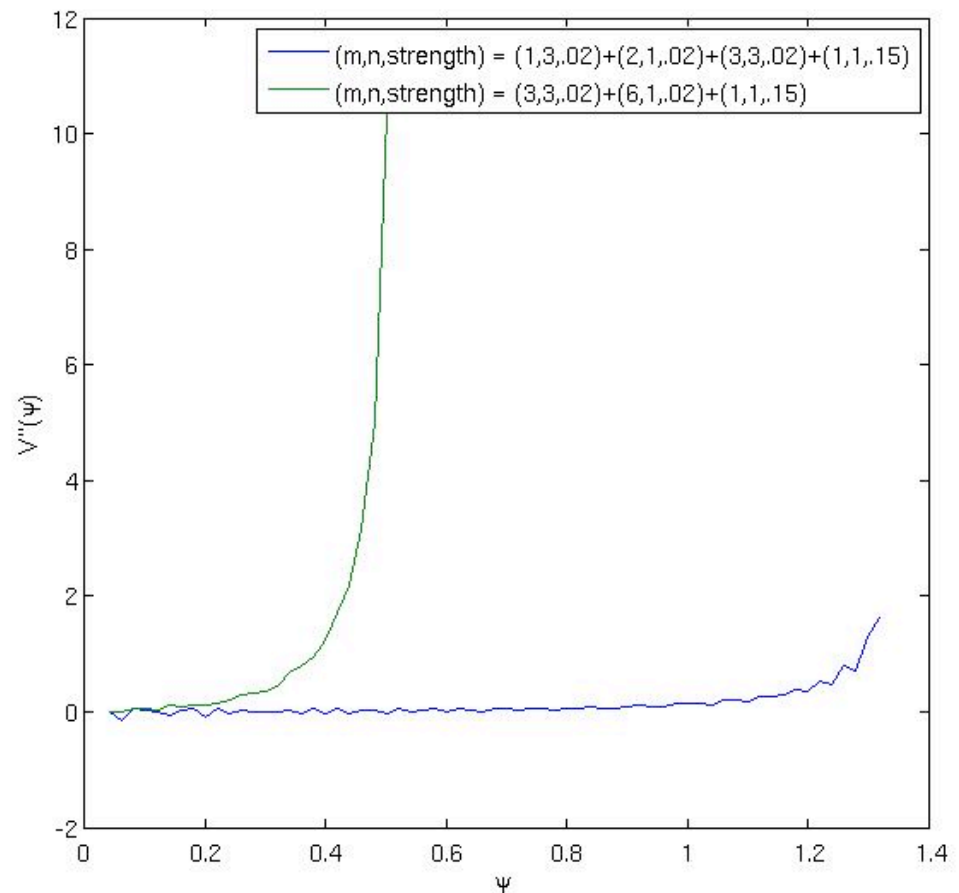
$$\varepsilon_{mn} \cdot t \cong \sum 2mn^3 \frac{\varepsilon_{mn}^2}{R^2} \left[\frac{1}{u} \left(\frac{I_m I_m'}{u} \right)' \right] \sim \sum \hat{t}_{mn} \left(\frac{r}{a} \right)^{2m-4}$$

- $m = 1$ rotating, helical axis, $m = 2$ nearly shearless, $m = 3$ has shear but no transform on axis, etc.

By using different combinations of magnetic harmonics, you can construct equilibria with different properties

- Ability to adjust various equilibrium properties
- V'' enters as an important parameter in resistive stability and isolated magnetic island calculations.

Example of the Variation in V'' for Different Mode Combinations



Solutions of the vacuum magnetic field are obtained and loaded into NIMROD

- The analytic vacuum solution is coded in straight cylinder geometry on NIMROD
 - New input variables were created to describe the strength of each helical harmonic. Any number of mode combos can be used.
 - A new subroutine was written (in physics_init.f) to cycle through all blocks, all cells and mode combinations. The routine calculates the field at each location, performs a fft and does a lagr_quad_basis_assign_loc to load the field.
 - At the grid boundary, the normal component of the magnetic field is NOT updated.
 - Implemented in NIMROD --- input vacuum field produced curl-free, divergence free magnetic field. Stable plasma state.

Good flux surfaces are initially formed.

Example: Poincare plots for $l=3, m=1$ helically symmetric magnetic field. These surfaces are shown for $t=0$.

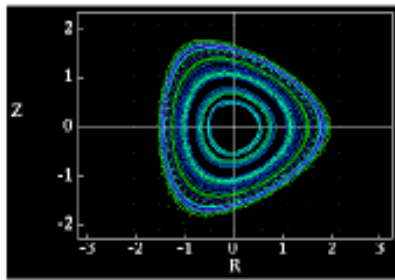


Figure 2: Poincare plot for $l=3, m=1$ at $z = 0$.

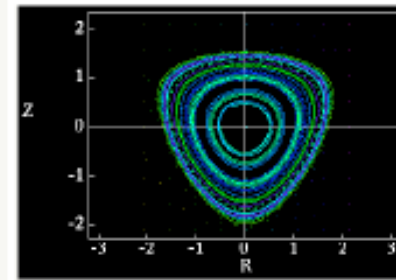


Figure 3: Poincare plot for $l=3, m=1$ at $z = L/4$.

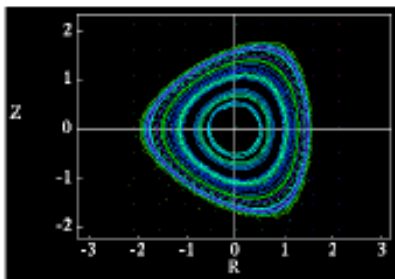


Figure 4: Poincare plot for $l=3, m=1$ at $z = L/2$.

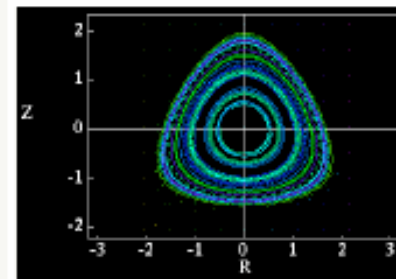


Figure 5: Poincare plot for $l=3, m=1$ at $z=3L/4$.



Good flux surfaces are seen to persist in initial NIMROD runs.

Example: Poincare plots for $l=3, m=1$ helically symmetric magnetic field. This initial vacuum magnetic field is then perturbed with a small shear Alfvén wave. These surfaces are shown for $t =$ one resistive time.

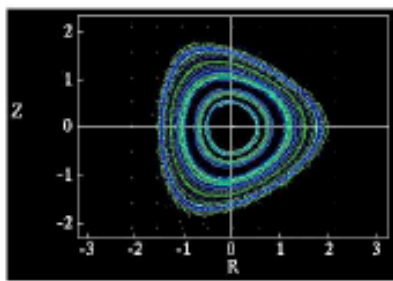


Figure 6: Poincaré plot for $l=3, m=1$ at $z = 0$.

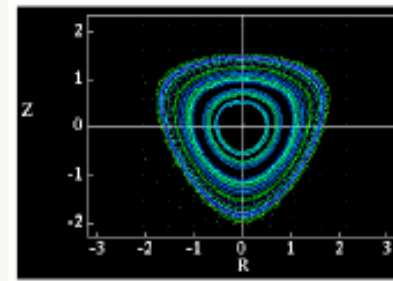


Figure 7: Poincaré plot for $l=3, m=1$ at $z = L/4$.

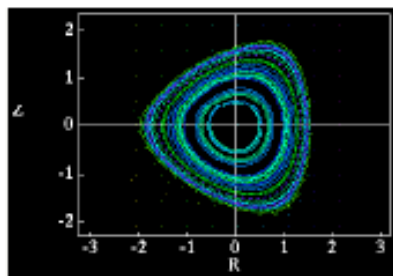


Figure 8: Poincaré plot for $l=3, m=1$ at $z = L/2$.

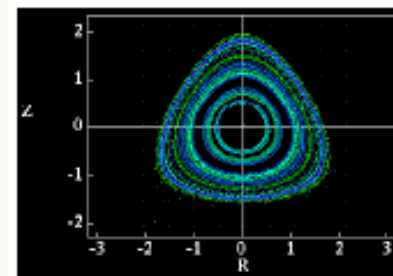


Figure 9: Poincaré plot for $l=3, m=1$ at $z=3L/4$.



Helically symmetric MHD equilibria can be generated

- 2-D solutions are available --- equilibrium fields are functions of two variables, r and $u = m\theta - n\zeta$. In

vacuum,

$$\vec{B} = B_0 \left[R_0 \zeta + \frac{nR_0}{m} \sum_{k=1} \varepsilon_k I_{km} \left(\frac{knr}{R_0} \right) \sin(ku) \right]$$

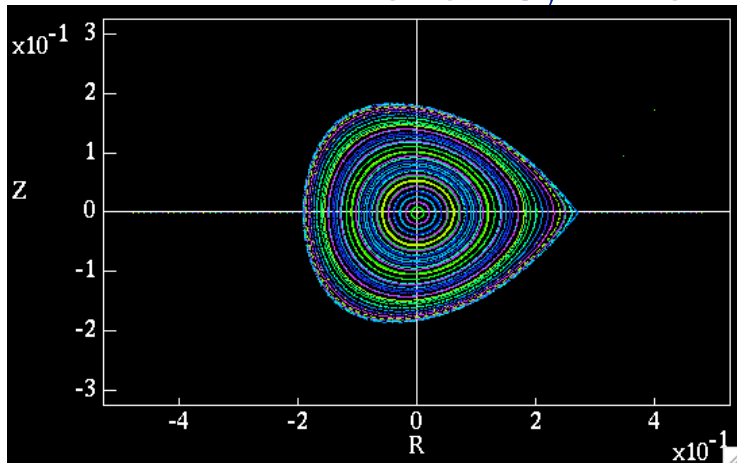
- Grad-Shafranov equation describes equilibrium

$$\Delta_h \psi = \frac{2nm/R_0}{m^2 + n^2 r^2 / R_0^2} f(\psi) - f \frac{df}{d\psi} - (m^2 + n^2 r^2 / R_0^2) \frac{dp}{d\psi},$$

$$\Delta_h = \frac{m^2 + n^2 r^2 / R_0^2}{r} \left[\frac{\partial}{\partial r} \frac{r}{m^2 + n^2 r^2 / R_0^2} \frac{\partial}{\partial r} + \frac{1}{r} \frac{\partial^2}{\partial u^2} \right]$$

For initial studies, two example 'equilibria' are employed

- Initially, two vacuum configurations are considered --- one with helical symmetry, one perturbed by a 3-D component

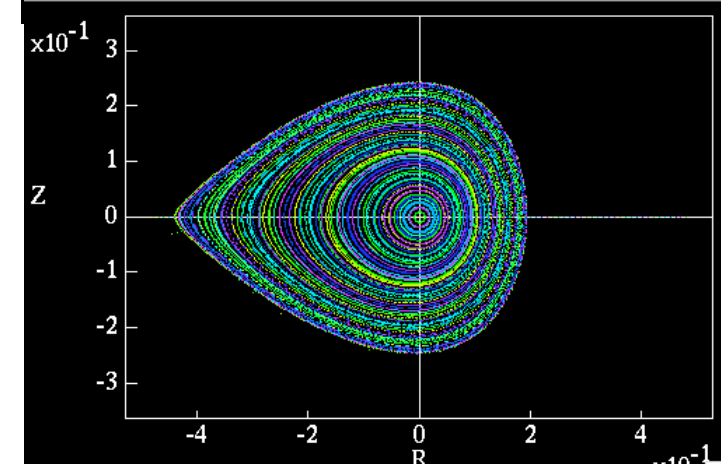
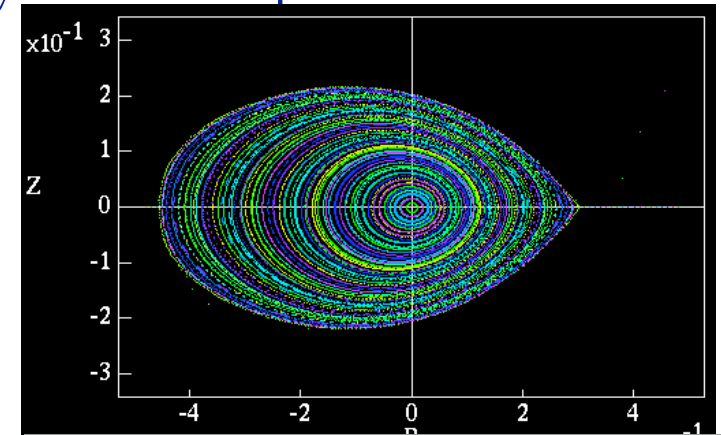
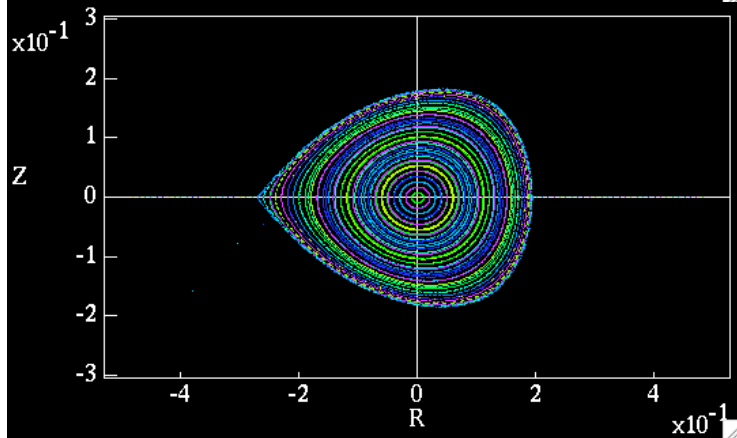


Flux
surfaces
at $t = 0$,
<- $z = 0$ ->

<- symmetric

w/ 3-D field ->

<- $z \neq 0$ ->

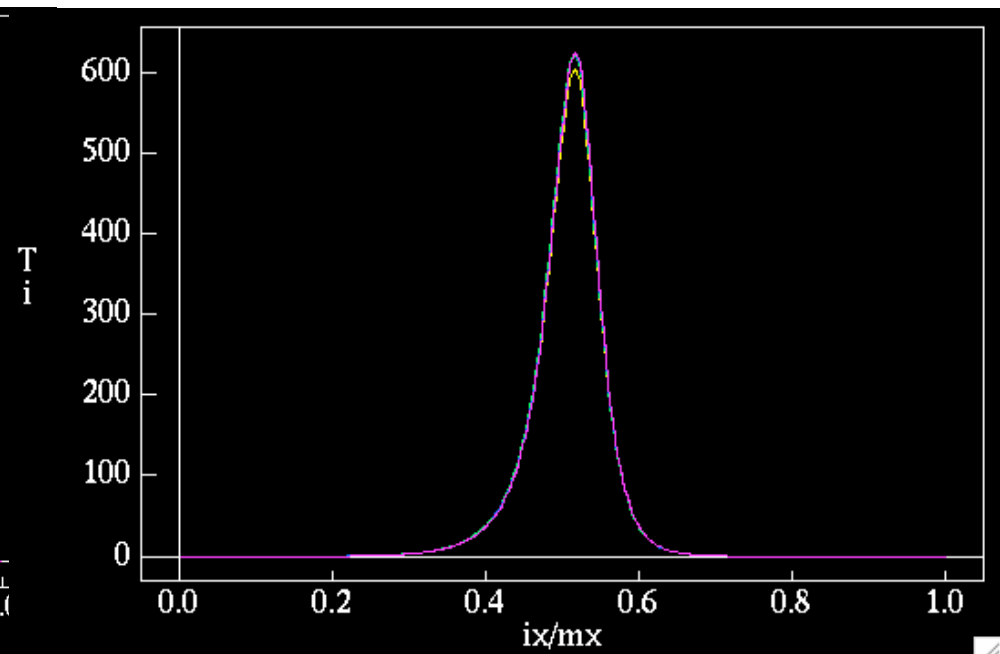
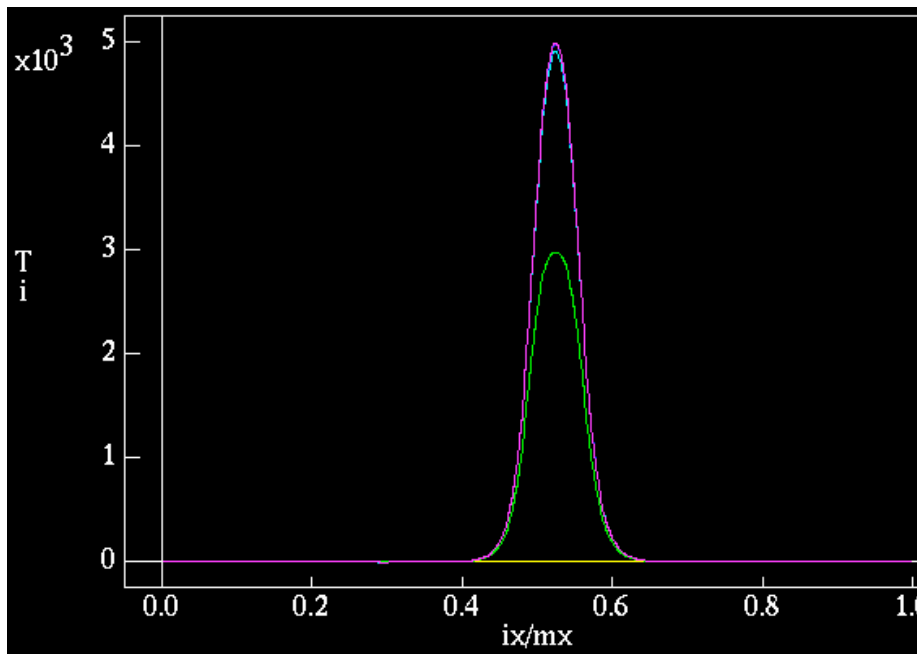


By adding a heating source, finite beta plasmas are generated

- Prescribed heating source and transport coefficients produce a temperature profile

Symmetric vacuum

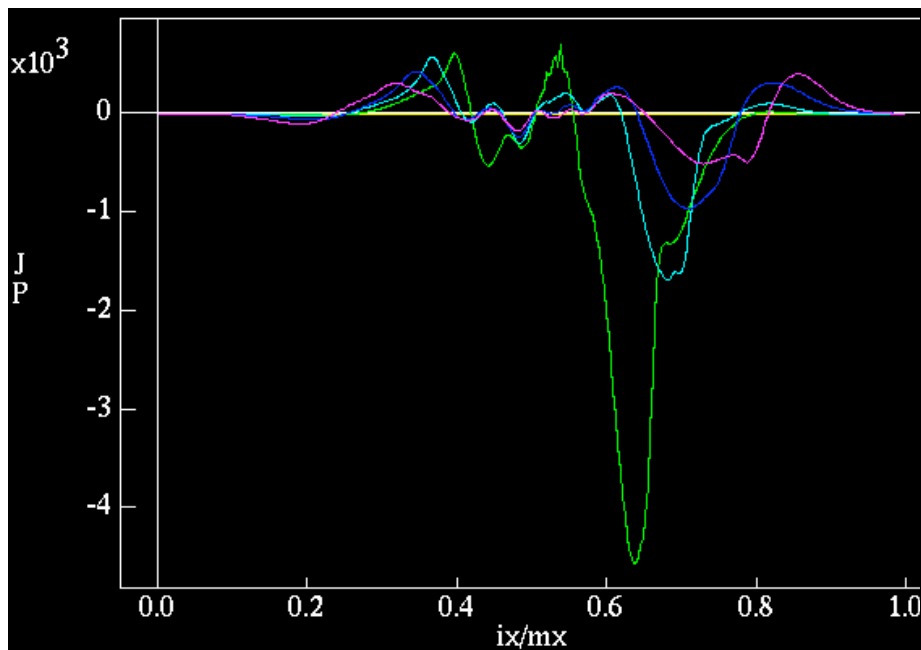
3-D vacuum



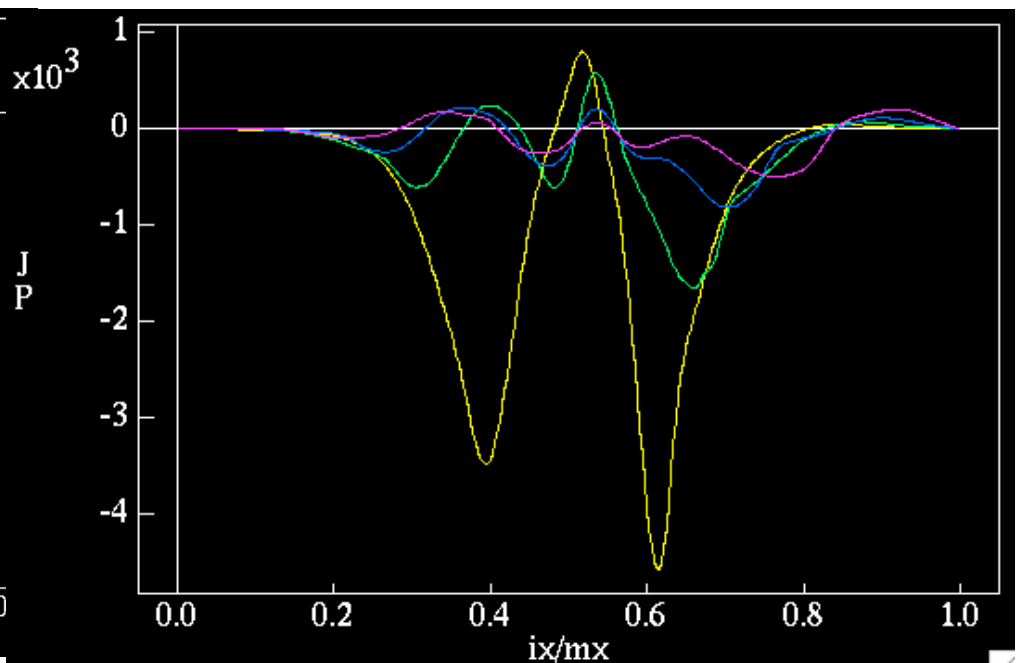
Self-consistent currents are calculated

- In equilibrium, currents are to diammagnetic and Pfirsch-Schluter effects. Transients apparent in the simulation

Symmetric vacuum

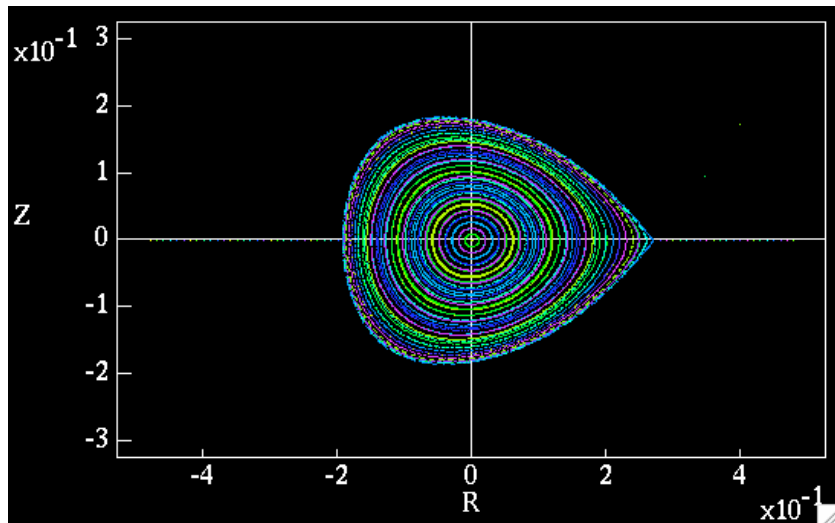


3-D vacuum

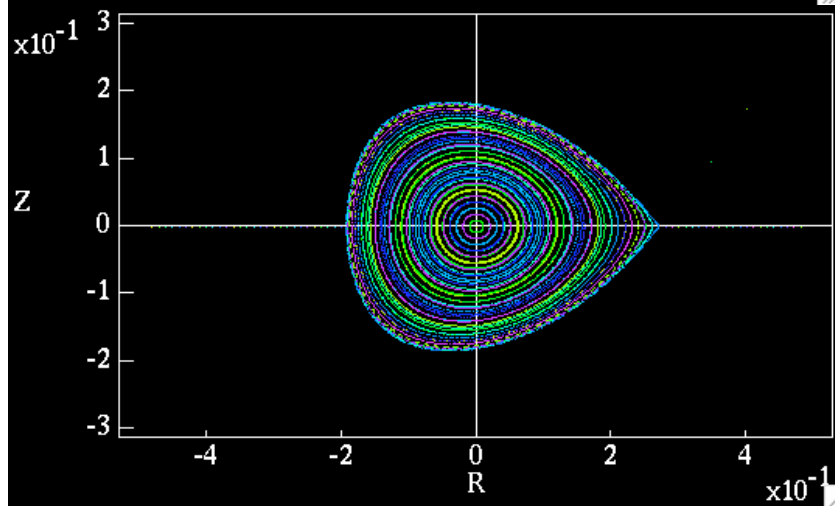


Initial simulations are low- β ; not a discernable effect on the equilibrium flux surfaces

2-D

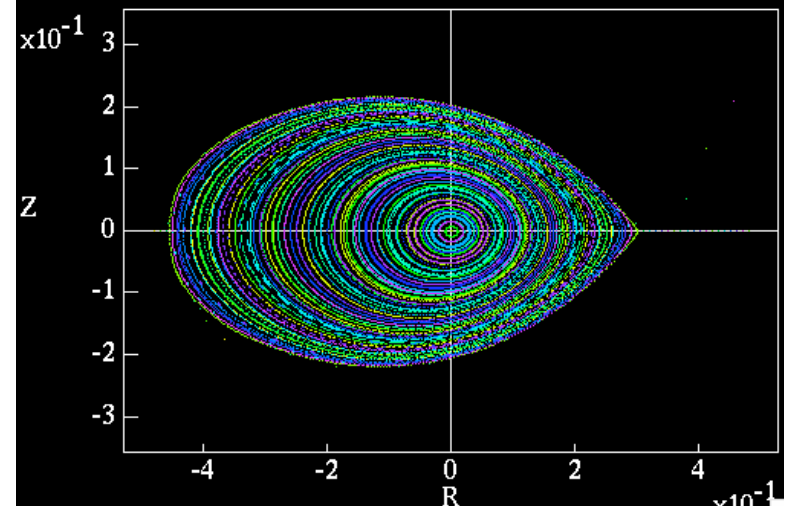
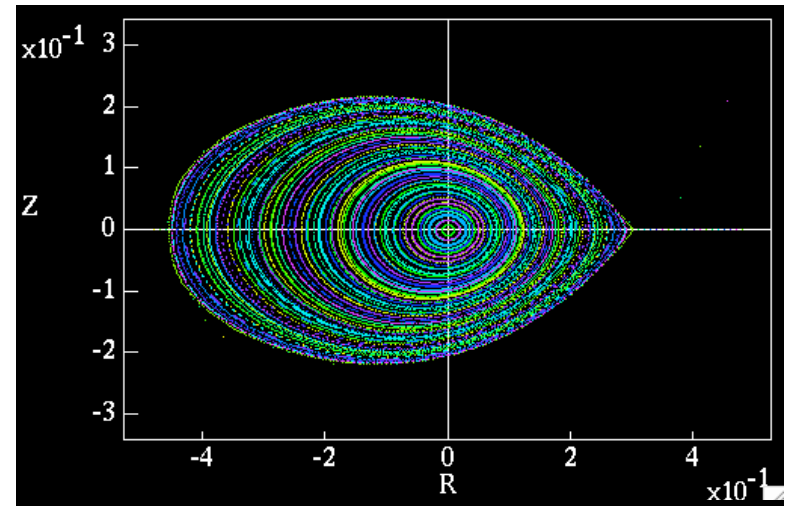


$t = 0$



$t = 800$

3-D



Future Plans

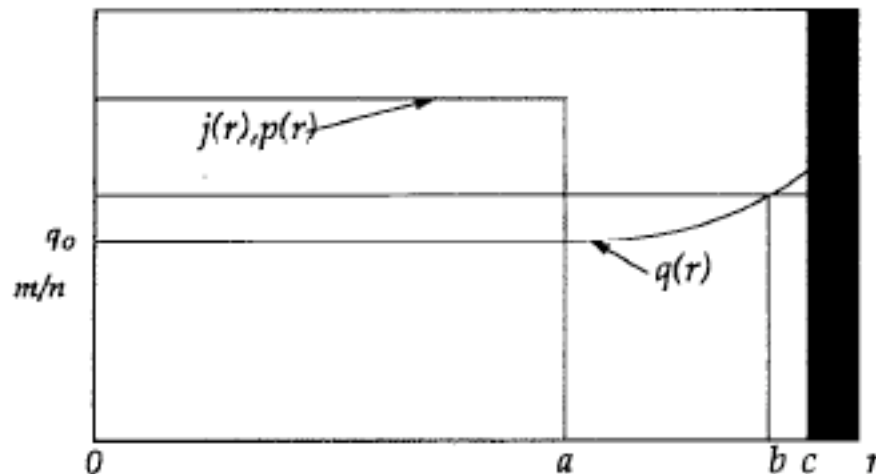
- Consistency of computed heated symmetric solutions with Grad-Shafranov theory.
- Lower dissipation
- Come up with a ‘standard’ heated symmetric base case which then can be perturbed.
 - Construct sequences of equilibria which vary rotational transform, gradient, V'' strength, etc.
- Temperature dependent transport coefficients.
- Resolution issues. Incorporate mixed finite elements.
- Multiple helicity cases with heating. Understand the role of transport physics on pressure induced islands/stochasticity, etc.
- Incorporate Held’s Chapman-Enskog-like closures.

Initial Studies of RWM, field error problems in a periodic cylinder --- A. Montgomery et al

- Motivation --- further the understanding of high- β tokamak physics in the presence of resistive walls, and field errors.
- Initially, a simple starter problem
- Eventually, high beta tokamak cases with plasma rotation, resistive wall and field error effects, non-zero resistivity (kink and tearing mode physics)

A starter problem has been identified

- Starter problem --- articulated in J. Finn, PoP (1995).
 - Reduced resistive MHD, periodic cylinder
 - flat current and pressure profile for $r \leq a$, diffuse plasma for $a < r \leq c$.
 - Thin resistive wall at $r = c$
 - Rigid rotation
- > Results obtained analytically

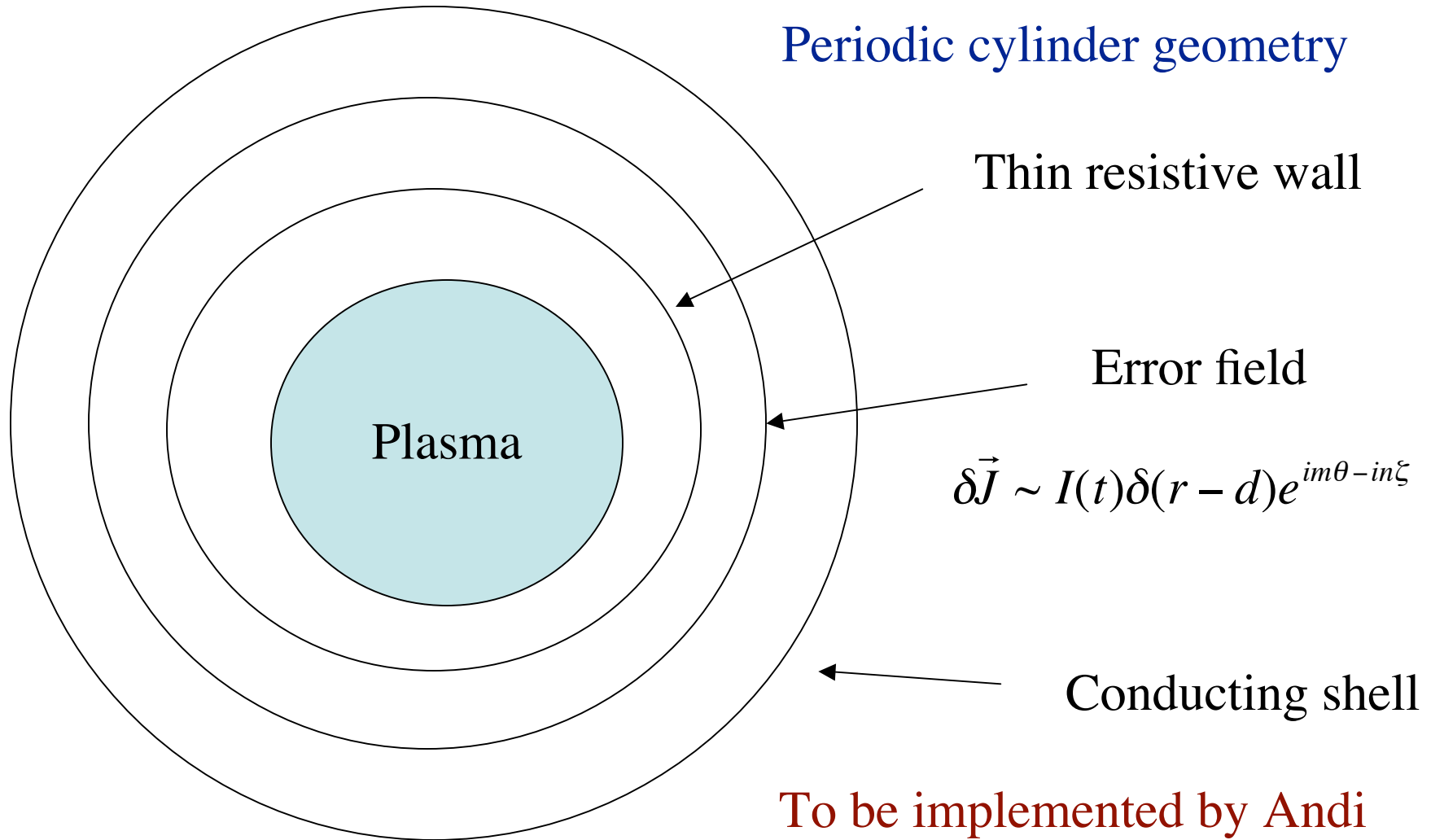


Transition between ideal to resistive mode is emphasized

- Results for a cylinder:
 - The existence of a RWM that cannot be stabilized by rigid plasma rotation in a cylinder depend critically on the lack of mode rational surfaces in the plasma.
 - Modes with rational surfaces in the plasmas are stabilized just below the ideal threshold by becoming resistive tearing modes. (Connection between ideal and resistive plasma modes.)
 - Tearing modes can be stabilized in the presence of a resistive wall and rotation
- Speculation that a similar effect occurs in a toroidal plasma--- yet to be explored

Starter problem geometry

Periodic cylinder geometry



$$\delta\vec{J} \sim I(t)\delta(r-d)e^{im\theta-in\xi}$$

To be implemented by Andi
with Scott K.'s and A. Cole's help